Eur J Transl Myol 34 (4) 12701, 2024 doi: 10.4081/ejtm.2024.12701

Longitudinal analysis of lower limb muscle activity and ankle tendon biosignals using structural equation modeling

Tatsuhiko Matsumoto,[1,2] Yutaka Kano[1]

[1]Graduate School of Engineering Science, Osaka University, Osaka; [2]Murata Manufacturing Co., Ltd., Kyoto, Japan.

Abstract

We collected biosignals from 63 participants and extracted the features corresponding to each level of exerted muscle force. Data were classified into typical and atypical patterns. Data analysis was performed using the Linear Latent Curve Model (LCM) and the Conditional Linear LCM. The typical patterns demonstrated a high degree of fit. Factors, such as ankle circumference and muscle mass, influenced the model intercept. A larger ankle circumference indicated attenuation of signal transmission from the tendon to the skin surface, leading to lower biosignal values. These results indicate that biosignals from the tendons near the ankle can be captured using piezoelectric film sensors. There are studies that define biosignals originating from tendons as mechanotendography. It has been demonstrated that the relationship between biosignals originating from tendons and the exerted muscle force can be explained linearly. Insights from this study may facilitate individualized approaches in the fields of motion control and rehabilitation. Physiological studies to elucidate the mechanisms underlying biosignal generation are necessary.

Key Words: lower limb muscle activity, tendon biosignals, longitudinal data, latent curve model, piezoelectric film sensor.

Eur J Transl Myol 34 (4) 12701, 2024 doi: 10.4081/ejtm.2024.12701

Human muscle activity quantification is a vital component in biomedical engineering research.[1,2] In motion control, lower limb muscle activity yields information on timing, patterns, and coordination, which illumines movement disorder mechanisms.[3,4] The evaluation of changes in muscle activity in cases of motor control abnormalities or movement disorders elucidates the mechanisms underlying these disorders.[5,6] In rehabilitation, this quantification provides insights into the overall activity and response speeds, facilitating the measurement of rehabilitation progress and contributing to plan optimization.[7,8] However, although electromyography (EMG) is widely employed for human muscle activity quantification, it necessitates placement of electrodes on the skin surface, which makes it unsuitable for long-term or intense physical activity measurements. To overcome these limitations, Isezaki *et al.* developed a sock-type wearable electromyograph.[9] Nevertheless, issues such as noise from sock sizing and sweatinduced interference between the electrodes and skin still require mitigation.

In this study, we shifted the focus to the tendons near the ankle joint and the biosignals they emit to circumvent the shortcomings of EMG signals. Tendons linked to muscles are known to emit signals associated with mechanical activities, such as mechanomyographic signals, and physiological tremors linked to the nervous system, both of which are useful for muscle activity quantification.[10,11] The ankle joint, which is a convergence point for tendons, such as the Achilles joint, and has minimal interference from fat and muscle, is an ideal site for biosignal acquisition. Consequently, we hypothesized that biosignals from the tendons near the ankle would be effective for quantifying lower limb muscle activity. Preliminary experiments using high-sensitivity piezoelectric film sensors placed on the Achilles tendon during isometric exercises indicated a correlation between the exercise intensity and sensor amplitude. Attempting to directly identify the mechanism behind these results would necessitate medical and physiological experimentation, which would involve considerable costs and risks. Hence, in this study, we posit a hypothesis that biosignals related to muscle activity originate from tendons near the ankle joint. Our aim is to indirectly corroborate this hypothesis through data science methods, allowing its plausibility to emerge.

We conducted data acquisition experiments and analyzed data from 63 participants. A data acquisition system

equipped with high-sensitivity piezoelectric film sensors was used to detect the biosignals at the ankle joint. The participants performed isometric exercises at four levels of muscle force exertion. The features of the piezoelectric film sensor that were correlated with the exerted muscle force were identified from the collected data. Longitudinal datasets, each consisting of four data points representing different exerted forces, were compiled for all the participants. Statistical models were fitted to evaluate the relationship between the identified features and exerted muscle force. In addition, we investigated the factors contributing to individual variations and their underlying mechanisms.

Materials and Methods

Experimental methods

Participants

A total of 63 healthy individuals aged 21– 58 years (31 males and 32 females) participated in the experiment. Prior to the experiment, the physical measurements of the participants (age, height, weight, body fat percentage, skeletal muscle mass, ankle circumference, and average grip strength) were recorded. The body fat percentage and skeletal muscle mass were measured using a bioelectrical impedance analysis scale (InBody S10; InBody, Tokyo, Japan). Ankle circumference was measured in the upper ankle. The average grip strength was calculated as the mean of four measurements (two from each hand).

Data acquisition system

We developed a system for acquiring biometric signals near the ankle joint. The system uses a biodegradable piezoelectric film sensor (Picoleaf®, Murata Manufacturing Co., Ltd.)[12] made of polylactic acid and is characterized by nonpyroelectric properties, making it less susceptible to body temperature. This feature allows for the generation of electric charges from material strain, enabling more accurate measurements. Furthermore, the sensor, owing to its high sensitivity and flexibility, could detect minute skin displacements and vibrational changes caused by tendon movements, regardless of body contours, making it valuable for biological applications. The system was designed such that a sensor was positioned on the side of the Achilles tendon.[13] The sampling frequency of the sensor was set to 1000 Hz.

Exercise protocol

The potential noise sources in this experiment are defined as follows: i) Experimental noise (noise that may occur during the experiment, such as body movements, system positioning, and participants not performing the exercises as intended); ii) Biological noise (noise that may arise owing to day-to-day variations in the physical and neurological properties of the participants).

The experimental protocol was designed such that biometric signals were obtained from ankle joints with minimal experimental and biological noise. A Cybex isokinetic dynamometer (Cybex NORM®, HUMAC, CA, USA) was used[14] to suppress experimental noise caused by body movements. The participants were seated in the dynanometer with the knee rotation axis (the lateral epicondyle of the femur) aligned with the machine axis. The knee angle was fixed at 90°, and the shin pad was secured just above the external malleolus. The ankle angle was fixed at 90°. The right foot was used for the measurements, regardless of the participant's dominant foot or hand, and was secured accordingly. The dynanometer was calibrated according to the manufacturer's recommendations before clinical trials. The experiment was structured into three phases. The warm-up phase was initially conducted with two objectives, to prevent physical abnormalities in participants during the test and to homogenize any heterogeneous physical and neurological properties, thereby reducing biological noise. In operation training phase, the researcher provided instructions to the participants. To ensure stable data acquisition, the participants were first secured to a Cybex machine and provided ample practice time (approximately 1 min) to become familiar with the operation. This was done to reduce the experimental noise that could arise from participants' failure to perform the exercises as intended. Data acquisition phase was placed after warm-up and operational training. Let i ($i = 1, \ldots, 4$) denote the exertion force number, j ($j = 1, \ldots, 63$) the participant ID, and p_{ij} ($p_{ij} = 25, 50, 75, 100$) the exertion force expressed as a percentage of each participant's MVC. Isometric plantar flexion movements of the ankle were performed, and data were acquired in the following order: MVC (100% MVC), 25% MVC load (25% MVC), 50% MVC load (50% MVC), and 75% MVC load (75% MVC). Data acquisition was conducted in three sets, each lasting for 5s. The dynamometer-measured torque values were displayed in real time on a monitor used by the participants to control the exertion force. The participants were instructed to gradually increase their exertion force over 10s with the goal of reaching the specified value at the 10-s mark. The experimenter also monitored and confirmed that the exerted force had reached a designated value before the measurement. A 20-s rest period was provided between each measurement set. The data acquisition system and procedure are illustrated in Figure 1.

Data preprocessing

Feature extraction

The amplitude of the sensor signal and the exerted muscle strength exhibited a directly proportional relationship. In fields such as acoustics and vibration, the magnitude of the amplitude is quantified using the root-mean-square (RMS) value.[15] We chose RMS as the feature for quantifying the amplitude. Let t ($1 \leq t \leq T_{ij}$) denote the time at which the raw data from the piezoelectric film sensor are acquired. If s_{ijt} represents the value of the piezoelectric film sensor signal at time t and RMS_{ij} is the RMS of the signal, the RMS can be defined by Equation (1).

$$RMS_{ij} = \sqrt{\frac{1}{T_{ij}} \sum_{t=1}^{T_{ij}} (s_{ijt})^2}. \quad (1)$$

Furthermore, in the fields of acoustics and vibration, the values are often expressed in decibels relative to a standard reference value.[16] A similar approach was adopted in the present study. The reference value RMS_0 was defined as the minimum RMS value obtained from the steady-state data of all participants, as shown in Equation (2).

$$RMS_0 = \min(\sqrt{(s_{ijt})^2}) \quad (2)$$

The RMS_0 value obtained from the experimental data was 2.44×10^{-5}. Therefore, the magnitude of the biosignal, expressed in dB, V_{ij} was calculated using Equation (3):

$$V_{ij} = 20 \log \left(\frac{RMS_{ij}}{RMS_0} \right) \quad (3)$$

Clustering

After preprocessing, the data were structured into longitudinal datasets with each participant j having a biosignal V_{ij} corresponding to the exerted muscle force p_{ij}. The difference in V_{ij} from the muscle force i to $i + 1$ was defined as ΔV_{kj} ($k = 1,...,3$). Curve patterns were classified based on ΔV_{kj} using the following procedure: i) Using density-based spatial clustering of applications with noise (DBSCAN), the patterns were classified into typical and atypical curve patterns based on the differences ΔV_{1j} (between 25% MVC and 50% MVC) and ΔV_{2j} (between 50% MVC and 75% MVC);[17] ii) After excluding typical curve patterns, the remaining curve patterns were reclassified using DBSCAN based on ΔV_{1j} and ΔV_{2j}, and it was manually determined which belong to typical curve patterns and which do not; iii) Typical curve patterns and others were classified using DBSCAN based on the difference ΔV_{3j} (between 75% MVC and 100% MVC).

The classification based on ΔV_{1j} and ΔV_{2j} was separated from that based on ΔV_{3j} because the former was part of an experiment in which participants controlled their exerted muscle force, whereas the latter was used for the maximum torque value assessment at 100% MVC. Thus, they potentially involved different types of noise. Figure 2 illustrates the clustering procedure and types of atypical patterns.

Data analysis methods

Structural equation modeling (SEM) is a versatile theoretical framework extensively used in various research fields, such as social sciences and medicine, to analyze causal models involving latent and observed variables.[18] The fundamental procedure in SEM involves creating models based on hypotheses and then selecting the optimal model by comparing the information criteria and fit

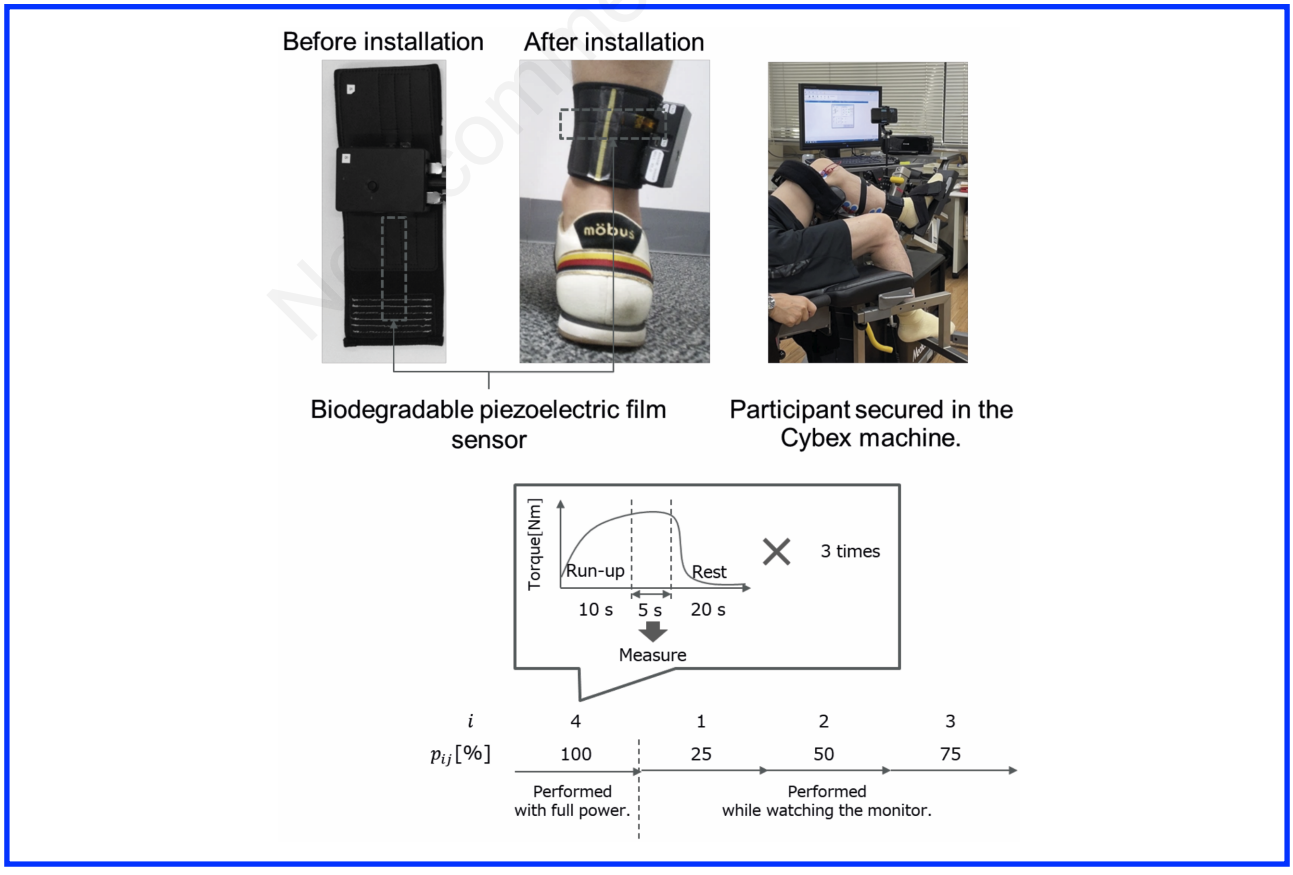

Figure 1. *Illustration of the biometric signal acquisition system, device placement on the body and procedure.*

indices, thereby identifying the true hypothesis. In this study, we evaluated four measures: the adjusted goodness of fit index (AGFI), comparative fit index (CFI), RMSE of approximation (RMSEA), and standardized root mean square residual (SRMR). AGFI and CFI values greater than 0.9 generally indicate a good model fit.[19,20] Similarly, RMSEA and SRMR values less than 0.08 are considered good, whereas values greater than 0.1 indicate a poor fit.[21,22] These indices define the fit differently; therefore, we report all of them here.

We based our analysis on the Latent Curve Model (LCM), which is well suited for longitudinal data.[23] The LCM is a statistical model designed to model longitudinal phenomena. It can estimate the trajectory of intra-individual changes over time and the inter-individual differences in these changes. Thus, it estimates parameters associated with time-variant general group tendencies and estimates the extent to which these parameters vary among individuals within a population simultaneously.

$$V_{ij} = \beta_{0j} + \beta_{1j} p_{ij} + r_{ij} \quad (4)$$

$$r_{ij} \sim N(0, \sigma^2) \quad (5)$$

$$\beta_{0j} = \gamma_{00} + u_{0j} \quad (6)$$

$$\beta_{1j} = \gamma_{10} + u_{1j} \quad (7)$$

$$(u_{0j}, u_{1j}) \sim MVN(\mathbf{0}, T) \quad (8)$$

$$T = \begin{bmatrix} \tau_{00} & \tau_{10} \\ \tau_{01} & \tau_{11} \end{bmatrix} \quad (9)$$

In this model, β_{0j} represents the random intercept, which, in our study, denotes the population mean of the biosignal magnitude for the participant j at 25% MVC exerted muscle strength p_{ij}. β_{1j} is the random slope indicating the average change in the dependent variable V_{ij} when the exerted muscle strength p_{ij} increases by 1%. The term r_{ij} is the residual error that represents the deviation of the measured value V_{ij} for each exerted muscle strength p_{ij} of participant j from $\beta_{0j} + \beta_{1j} p_{ij}$. Equation (5) indicates that the deviation r_{ij} follows a normal distribution with zero mean and variance σ^2. This model includes various assumptions when approached using SEM. For example, explanatory variables for the random intercept denoted as $x^{(l)}_{0j}$ and those for the random slope denoted as $x^{(m)}_{1j}$, with l and m representing the number of explanatory variables, can be added to equations (6) and (7) to transform them into equations (10) and (11), respectively, resulting in a conditional LCM. Equations (10) and (11)

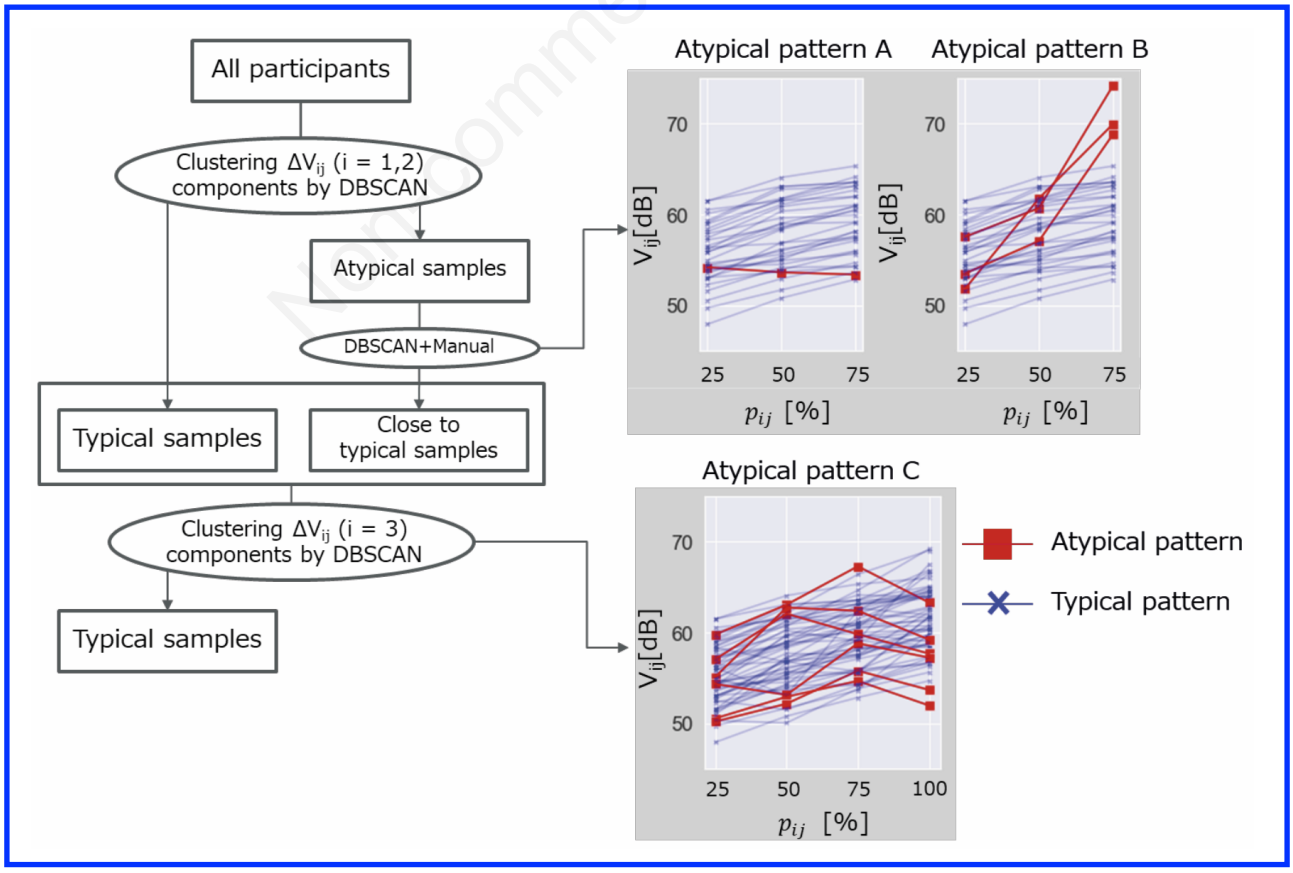

Figure 2. *Clustering procedure and illustration of atypical patterns.*

allows us to focus on explaining interindividual differences.[24,25]

$$\beta_{0j} = \gamma_{00} + \gamma_{01} x_{0j}^{(l)} + u_{0j} \quad (10)$$

$$\beta_{1j} = \gamma_{10} + \gamma_{11} x_{1j}^{(m)} + u_{1j} \quad (11)$$

Results

Linear LCM

Path diagram is presented in Figure 3. Equalvariance constraints are applied to the variances of V_{1j}, V_{2j}, and V_{3j}, whereas V_{4j} is treated separately. This decision is based on the different types of noise involved, as discussed in Section II-B.2.

Table 1 displays the fit indices and the parameters using only typical pattern data. Overall, these indices indicate a good fit. The CFI and AGFI reflect the overall fit of the proposed model to the observed data, while the RMSEA and SRMR highlight the discrepancies, uncertainties, and error rates between the actual observations and predictions. The results were favorable based on both sets of indices.

Additionally, the estimated average intercept γ_{00} was 53.392, and the average slope γ_{10} was 0.083. The 95% confidence interval for the slope was positive, indicating that the biosignal V_{ij} tended to increase monotonically on average, as the exerted muscle strength p_{ij} increased. This monotonic increase was quantified in increments of 0.083 for each 1% increase in p_{ij}. Moreover, the variance in the slope τ_{11} was 0.001. The slope distribution was assumed to follow a normal distribution, as indicated in Equation (5), suggesting that the biosignal V_{ij} increased monotonically with the exerted muscle strength p_{ij}, regardless of interindividual differences.

Conditional linear LCM

A conditional linear LCM was constructed using participant-specific information to estimate intercepts and slopes. Participant-specific information was selected after removing multicollinearity through a stepwise variable increase and decrease method based on the Akaike information criterion.

Although the SRMR value was slightly high (0.092), the AGFI, CFI, and RMSEA indices indicated a good fit. This implies that although the model fit the data well, there is potential for improvement through structural adjustments or consideration of additional variables. Overall, the model demonstrated high reliability. The estimated value of the explained variance, PVE(τ_{00}) was 0.421, which indicates that the explanatory variables for the intercept could explain 42.1% of the individual variance. Therefore, the selected explanatory variables contributed significantly to the estimation of the biosignal value at 25% MVC.

Table 2 lists the explanatory variables selected for the intercepts and slopes. The selected explanatory variables for the intercept were the sensor value at steady state (0% MVC), maximum torque value at 100% MVC, ankle circumference, and average grip strength. All the variables contributed significantly to the intercept estimation when a two-tailed t-test is conducted at the 5% significance level. The most influential variable was the maximum torque value at 100% MVC, with a regression coefficient of 0.063, indicating that the intercept fluctuated by ±2.64 based on this variable. The other variables also significantly influenced the intercept: the sensor value at the steady state (±2.27), ankle circumference (±1.78), and average grip strength (±2.03). However, none of the variables significantly affected the slope.

Comparison of typical and atypical patterns

Figure 4 presents a box plot that illustrates the distribution of the physical and experimental data for all participants and the information of the participants classified as having atypical patterns. The box represents the interquartile

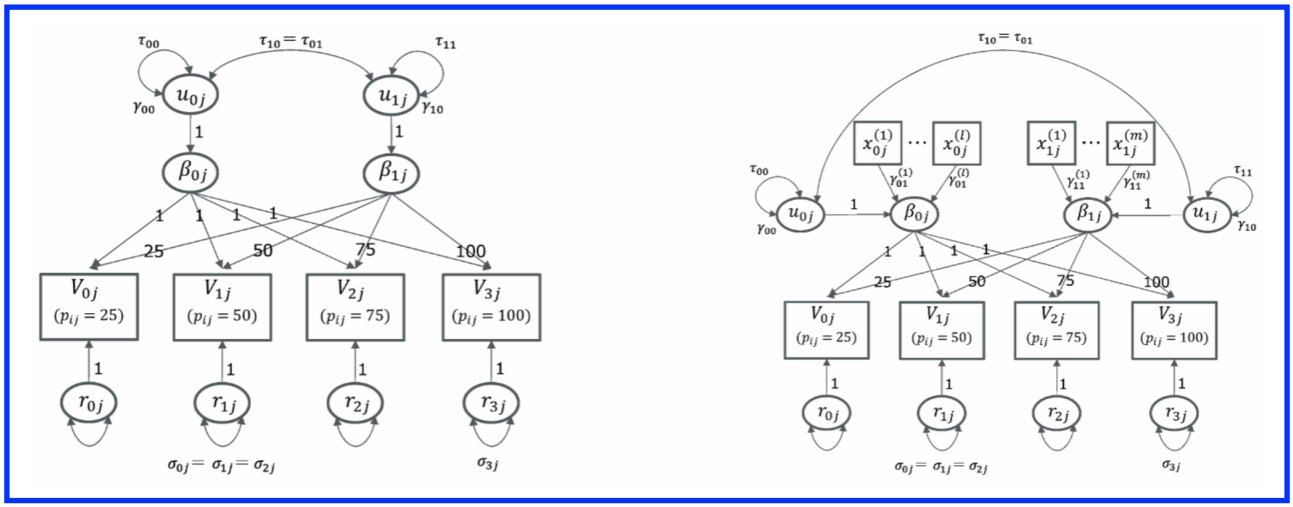

Figure 3. *Path diagram for the linear LCM and conditional linear LCM.*

range of the dataset and the whiskers extend to cover the remainder of the distribution. We denote the first quartile by Q_1, the third quartile by Q_3, and the interquartile range by IQR = $Q_3 - Q_1$. The lower and upper whiskers extend to the minimum value within $Q_1 - (1.5 \times \text{IQR})$ and maximum value within $Q_3 + (1.5 \times \text{IQR})$, respectively. Data points outside these ranges were plotted as outliers. The overall distribution of the participants did not show significant differences in terms of age between males and females.

The participant with atypical pattern A, showing a monotonic decrease, was a male with short stature and a lean body type. Participants with atypical pattern B, showing a larger increase in the biosignal value relative to the exerted muscle strength, included two males and one female. One of the males had a higher height, weight, body fat percentage, and maximum torque at 100% MVC. Participants with atypical pattern C, in which the biosignal values tended to decrease during 100% MVC, included two males and four females. One male patient had an ankle circumference notably larger than his physique. Among the females, one had a larger ankle circumference, higher BMI, and body fat percentage. The participants, regardless of gender, exhibited high maximum torque values at 100% MVC. Additionally, four of the five participants with pattern C had notable experimental notes, including

Table 1. *Parameters and Fit Indices of Linear LCM and Conditional Linear LCM.*

Model parameter	Linear LCM Estimate	Linear LCM Standard error	Linear LCM 95% confidence intervals	Conditional linear LCM. Estimate	Conditional linear LCM. Standard error	Conditional linear LCM. 95% confidence intervals
γ_{00}	53.392	0.501	[52.400, 54.383]	41.784	5.991	[29.921, 53.646]
γ_{10}	0.083	0.005	[0.0073, 0.0092]	0.083	0.005	[0.073, 0.092]
τ_{00}	11.079	-	-	6.414	-	-
$\tau_{10}=\tau_{01}$	-0.041	-	-	-0.037	-	-
τ_{11}	0.001	-	-	0.001	-	-
$\sigma^2_{1\text{-}3}$	1.377	-	-	1.386	-	-
$\sigma^2_{1\text{-}3}$	2.125	-	-	2.069	-	-
PVE(τ_{00})	-	-	-	0.421	-	-

	Fit indices for the linear LCM							Fit indices for the linear LCM						
	χ^2	df	p-value	AGFI	CFI	RMSEA	SRMR	χ^2	df	p-value	AGFI	CFI	RMSEA	SRMR
	8.39	7	0.298	0.999	0.993	0.061	0.068	27.65	19	0.090	0.998	0.963	0.052	0.092

Table 2. *Explanatory variables selected for the intercept and slope of the conditional LCM.*

	Explanation variablefor intercept	Intercept	Variance	Estimate	Standard error	p-value
$x^{(l)}_{0j}$	Sensor value at steady [dB]	49.577	13.427	0.317	0.089	0.000
	Torque value at MVC [N·m]	53.660	458.074	0.063	0.019	0.001
	Ankle circumference [cm]	21.586	3.294	-0.501	0.197	0.011
	Average grip strength [kg]	33.610	108.262	0.100	0.040	0.013
$x^{(l)}_{1j}$	All variables non-significant based on variable selection					

changes in foot fixation settings or unstable torque values during the experiment.

Discussion and implications

Factors contributing to inter-individual differences

When examining the explanatory variables for the intercept, it was observed that a larger ankle circumference resulted in a lower intercept value. This outcome aligns with the hypothesis that biosignals generated by tendons attenuate before reaching the skin surface and that this attenuation is proportional to the distance from the tendon to the skin surface. This hypothesis is consistent with the finding that higher steady-state sensor values lead to higher intercepts.

Furthermore, higher maximum torque values at 100% MVC were associated with higher intercept values. Generally, individuals with higher maximum torque values are more likely to have greater muscle mass. At 25% MVC, individuals with a greater muscle mass can mobilize more muscles. Consequently, more muscle activation leads to higher biosignal quantities, which explains why individuals with higher maximum torque values at 100% MVC had higher intercept values. This hypothesis is also consistent with the finding that higher average grip strength leads to higher intercept values.

Factors contributing to atypical patterns

Further analysis was conducted for participants with atypical pattern C, who showed a decreasing trend, especially at p_{4j}. Among the five participants identified as exhibiting pattern C, participants with IDs 109 and 114 displayed exceptionally high maximum torque values at 100% MVC. Such high values indicate that the participants used synergistic muscles (such as quadriceps) in addition to the primary muscles during the dynamometer test. In this scenario, the combined torque values were recorded as the maximum torque at 100% MVC. Consequently, the torque settings for p_{1j} to p_{3j} were set to be higher than the actual abilities of the participants, resulting in higher values of V_{1j} to V_{3j}. However, the activation of synergistic muscles can reduce the activity of the primary muscles.[26] If V_{4j} represents the activity of the primary muscles, it exhibits lower values. The average grip strength of these two participants with IDs 109 and 114 supports the hypothesis that the maximum torque values at 100% MVC include the force from the synergistic muscles. Furthermore, changes in the fixation methods during an experiment can alter the contribution of synergistic muscles.[27] The control of the primary muscles also affects the ratio of the primary and synergistic muscle contributions. These phenomena were observed in the experimental notes of four of the five participants, suggesting that the high maximum torque

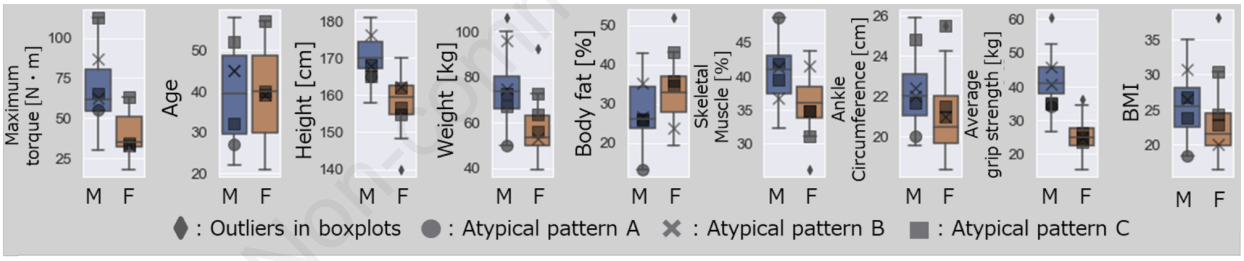

Pattern	ID	Sex	Maximum torque [N · m]	Age	Height [cm]	Weight [kg]	Body fat [%]	Skeletal muscle [%]	Ankle circumference [cm]	Average grip strength [kg]	BMI (Body mass index)	Experimental notes
A	110	M	55	27	165.0*	50.0**	13.2**	48.8**	20.0*	34.1*	18.3**	-
B	126	M	62	45	167.8	74.5	26.5	41.3	22.0	45.7	26.4	-
	129	M	87*	45	176.3*	95.7*	35.1*	36.6*	22.4	40.5	30.7*	-
	118	F	33	39	162.1	52.8	23.7*	41.4*	21.0	24.7	20.0	-
C	109	M	113**	32	168.0	67.0	26.0	39.4	21.7	34.9*	23.7	Unstable torque values during 75% MVC.
	130	M	65	52*	165.0*	72.8	25.7	41.8	24.8*	25.0*	26.7	Changing the foot fixation setting from 75% MVC.
	114	F	63**	39	161.8	63.5*	35.7	34.8	21.0	24.9	24.2	Changing the foot fixation setting from 50% MVC.
	146	F	33	57**	154.7*	72.9**	43.0**	31.0	25.5***	23.4	30.4**	Unstable torque values during 100% MVC.
	161	F	34	40	156.5	55.9	34.7	34.8	21.5	26.3	22.8	-

* $> Q_3$ or $< Q_1$.
** Lower whisker value or upper whisker value.
*** Outliers in box plots.

Figure 4. *Box plot of participant's physical information and participants information for atypical patterns.*

values at 100% MVC included forces from the synergistic muscles. Thus, atypical pattern C can be attributed to experimental noise owing to the unintended use of synergistic muscles during the 100% MVC tests. This also implies the validity of excluding pattern C from the model.

Relationship between biosignals and mechanotendography

The analysis revealed that the slopes, including the 95% confidence intervals, are positive for both the latent growth model and the conditional latent growth model. Specifically, the positivity of the slopes in the conditional latent growth model suggests that, for both genders, the biosignal V_{ij} increases monotonically on average with the increase in muscle strength p_{ij}. This study assumes the presence of biosignals originating from tendons, which Schaefer et al. have defined and reported as mechanotendography.[28,29] Although they assumed biosignals akin to acoustic signals, they considered lower frequencies and used the same piezoelectric sensors as we did. The biosignals dealt with in this study are likely related to mechanotendography as studied by Schaefer *et al.* To date, no study has verified the trends of mechanotendography under multi-level isometric contraction loads. This study suggests that mechanotendography can contribute not only to the detection of muscle activity levels but also to their quantification. Future research needs to investigate the relationship with the mechanotendography defined by Schaefer *et al.*

Conclusions

In this study, the biosignals originating from the tendons near the ankle joint were used for limb muscle activity quantification. We conducted data acquisition experiments and analyses on 63 participants to capture biosignals from the ankle joint and extract features corresponding to the exerted muscle forces. For typical patterns, modeling was performed using a linear LCM and a conditional linear LCM. The linear LCM for typical patterns showed high potential for linearly explaining the relationship between the exerted muscle forces and biosignals. Conditional linear LCM revealed that physical information, such as ankle circumference and average grip strength, influenced the intercept of the model.

This study demonstrated that the relationship between the biosignals and exerted muscle forces can be explained by a simple linear structure, which is advantageous for estimating exerted muscle forces using biosignals. Additionally, participant-specific physical information can be used to adjust for individual biases. These results increase the feasibility of realizing a generalized model for estimating exerted lower limb muscle forces.

We plan to analyze the relationship between the EMG signals and biosignals captured in this study to further demonstrate the efficacy of biosignals. Further experiments will be conducted under different conditions to validate the applicability of this method to other muscles and areas of motion. Experiments to elucidate the mechanisms underlying biosignal generation should also be conducted from a physiological perspective.

List of abbreviations

EMG, Electromyography
RMS, Root mean square
MVC, Maximal voluntary contraction
SEM, Structural equation modeling
LCM, Latent curve model
AGFI, Adjusted goodness of fit index
CFI, Comparative fit index
RMSEA, Root mean square error of approximation
SRMR, Standardized root mean square residual
PVE, Proportions of variance explained
IQR, Interquartile range

Conflict of interest

The authors declare that they have no financial or non-financial conflicts of interest related to the content of this manuscript.

Funding

This study did not receive any funding in any form.

Ethics approval and consent to participate

The experimental protocol was performed according to the principles of the Declaration of Helsinki. Informed consent was obtained from all the participants prior to the experiment, and the study was approved by the Ethics Committee of Shikoku Medical School (Approval Number: R05-08-002).

Consent for publication

Not applicable.

Availability of data and material

The dataset used and/or analysed during the current study are available from the corresponding author on reasonable request.

Acknowledgments

We extend our deepest gratitude to Yuichi Motohisa and Nozomi Matsunaga of the Nagai Cardiovascular Internal Medicine Clinic and Chiharu Fujisawa from Shikoku Medical School for their invaluable cooperation and support. The expertise and dedication of these individuals were instrumental in the successful completion of our experiments and fundamental to achieving the profound insights gained from this research. We would also like to express our appreciation to Atsushi Naito, Naoki Kawara, Yutaka Takamaru, and Risako Yamashita from Murata Manufacturing

Co., Ltd. for their assistance and expertise, which contributed significantly to our research. We would like to thank Editage (www.editage.jp) for the English language editing.

Corresponding author

Tatsuhiko Matsumoto, Osaka University, 1-3, Machikaneyama, Toyonaka, Osaka, Japan.
ORCID ID: 0009-0003-4423-9718
E-mail: tatsuhiko.matsumoto@murata.com

Yutaka Kano
ORCID ID: 0000-0001-7323-1772
E-mail: kano.yutaka.es@osaka-u.ac.jp

References

1. Powell KE, Paluch AE, Blair SN. Physical activity for health: What kind? how much? how intense? on top of what? Ann Rev Public Health 2011;32:349-365.
2. Howard RM, Conway R, Harrison AJ. A survey of sensor devices: use in sports biomechanics. Sports Biomechanics 2016;15:450-461.
3. Walter JP, Kinney AL, Banks SA, et al. Muscle synergies may improve optimization prediction of knee contact forces during walking. J Biomech Engin 2014;136:021031.
4. Hansen C, Teulier C, Micallef JP, et al. Lower limb muscle activity during first and second tennis serves: a comparison of three surface electromyography normalisation methods. Sports Biomech 2023;1-12.
5. Schmitz A, Silder A, Heiderscheit B, et al. Differences in lower-extremity muscular activation during walking between healthy older and young adults. J Electromyography Kinesiol 2009;19:1085-91.
6. Arendt-Nielsen L, Graven-Nielsen T, Svarrer H, Svensson P. Influence of low back pain on muscle activity and coordination during gait: A clinical and experimental study. Pain 1996;64:231-240.
7. Farthing JP, Chilibeck PD. The effects of eccentric and concentric training at different velocities on muscle hypertrophy. Eur J Appl Physiol 2003;89:578-86.
8. Ekstrom RA, Donatelli RA, Carp KC. Electromyographic analysis of core trunk, hip, and thigh muscles during rehabilitation exercises. J Orthopaedic Sports Physical Ther 2007;37:754-62.
9. Isezaki T, Kadone H, Niijima A, et al. Sock-type wearable sensor for estimating lower leg muscle activity using distal EMG signals. Sensors 2019;19:1954.
10. Stokes MJ, Dalton PA. Acoustic myography for investigating human skeletal muscle fatigue. J Appl Physiol 1991;71:1422-6.
11. Koster B, Lauk M, Timmer J, et al. Central mechanisms in human enhanced physiological tremor. Neuroscience Letters 1998;241:135-8.
12. Ando M, Kawamura H, Kitada H, et al. Pressure-sensitive touch panel based on piezoelectric poly (l-lactic acid) film. Japanese J Appl Physics 2013;52:09KD17.
13. Jomyo S, Furui A, Matsumoto T, et al. A wearable finger-tapping motion recognition system using biodegradable piezoelectric film sensors. In: 2021 43rd Annual International Conference of IEEE Engineering in Medicine Biology Society (EMBC). IEEE, 2021.
14. Menegaldo LL, de Oliveira LF. Effect of muscle model parameter scaling for isometric plantar flexion torque prediction. J Biomech 2009;42:2597-2601.
15. Immovilli F, Bianchini C, Cocconcelli M, et al. Bearing fault model for induction motor with externally induced vibration. IEEE Transactions on Industrial Electronics 2012;60:3408-3418.
16. Tsypkin M. Induction motor condition monitoring: Vibration analysis technique-a twice line frequency component as a diagnostic tool. In: 2013 International Electric Machines Drives Conference, 2013. p. 117-124.
17. Ester M, Kriegel HP, Sander J, Xu X. A density-based algorithm for discovering clusters in large spatial databases with noise. In: KDD, 1996. p. 226-231.
18. Hox JJ, Bechger TM. An introduction to structural equation modeling. In: Partial Least Squares Structural Equation Modeling (PLS-SEM) Using R: A Workbook, 2021. p. 1-29.
19. Hoelter JW. The analysis of covariance structures: Goodness-of-fit indices. Sociological Methods Research 1983;11:325-344.
20. Cole DA. Utility of confirmatory factor analysis in test validation research. J Consulting Clin Psychol 1987;55:584.
21. Steiger JH. Understanding the limitations of global fit assessment in structural equation modeling. Personal Individual Diff 2007;42:893-8.
22. Iacobucci D. Structural equations modeling: Fit indices, sample size, and advanced topics. J Consumer Psychol 2010;20:90-8.
23. McArdle JJ, Grimm KJ. Five steps in latent curve and latent change score modeling with longitudinal data. In: Longitudinal Research with Latent Variables, 2010. p. 245-273.
24. Bollen KA, Curran PJ. Latent curve models: a structural equation perspective. Wiley and Sons, 2006.
25. Lance CE, Vandenberg RJ, Self RM. Latent growth models of individual change: The case of newcomer adjustment. Organizat Behav Human Decision Processes 2000;83:107-40.
26. Kubota K, Yokoyama M, Hanawa MT, et al. Muscle co-activation in the elderly contributes to control of hip and knee joint torque and endpoint force. Sci Rep 2023;13:7139.
27. Billot M, Simoneau EM, Ballay Y, et al. How the ankle joint angle alters the antagonist and agonist torques during maximal efforts in dorsi-and plantar flexion. Scandinavian J Med Sci Sports 2011;21:e273-81.
28. Schaefer LV, Bittmann FN. Mechanotendography: description and evaluation of a novel method for investigating the physiological mechanical oscillations of tendons using a piezo-based measurement system. Eur J f Translat Myol 2021;31:1.
29. Schaefer LV, Bittmann FN. Two forms of isometric muscle function: Interpersonal motor task supports a distinction between a holding and a pushing isometric muscle action. BioRxiv 2020;2020:08.

Eur J Transl Myol 34 (4) 12701, 2024 doi: 10.4081/ejtm.2024.12701

Disclaimer

All claims expressed in this article are solely those of the authors and do not necessarily represent those of their affiliated organizations, or those of the publisher, the editors and the reviewers. Any product that may be evaluated in this article or claim that may be made by its manufacturer is not guaranteed or endorsed by the publisher.

Submitted: 1 June 2024.
Accepted: 1 August 2024.
Early access: 23 September 2024.